The EMBO Journal (2011) 30, 823–834 | © 2011 European Molecular Biology Organization | Some Rights Reserved 0261-4189/11
www.embojournal.org

THE EMBO JOURNAL

EMBO open

Small RNA-mediated regulation of iPS cell generation

Zhonghan Li[1,2], Chao-Shun Yang[1,2], Katsuhiko Nakashima[2] and Tariq M Rana[1,2,*]

[1]Program for RNA Biology, Sanford-Burnham Medical Research Institute, La Jolla, CA, USA and [2]Department of Biochemistry and Molecular Pharmacology, University of Massachusetts Medical School, Worcester, MA, USA

Somatic cells can be reprogrammed to an ES-like state to create induced pluripotent stem cells (iPSCs) by ectopic expression of four transcription factors, Oct4, Sox2, Klf4 and cMyc. Here, we show that cellular microRNAs (miRNAs) regulate iPSC generation. Knock-down of key microRNA pathway proteins resulted in significant decreases in reprogramming efficiency. Three miRNA clusters, miR-17∼92, miR-106b∼25 and miR-106a∼363, were shown to be highly induced during early reprogramming stages. Several miRNAs, including miR-93 and miR-106b, which have very similar seed regions, greatly enhanced iPSC induction and modulated mesenchymal-to-epithelial transition step in the initiation stage of reprogramming, and inhibiting these miRNAs significantly decreased reprogramming efficiency. Moreover, miR-iPSC clones reached the fully reprogrammed state. Further analysis revealed that Tgfbr2 and p21 are directly targeted by these miRNAs and that siRNA knock-down of both genes indeed enhanced iPSC induction. Here, for the first time, we demonstrate that miR-93 and its family members directly target TGF-β receptor II to enhance iPSC generation. Overall, we demonstrate that miRNAs function in the reprogramming process and that iPSC induction efficiency can be greatly enhanced by modulating miRNA levels in cells.

The EMBO Journal (2011) **30,** 823–834. doi:10.1038/emboj.2011.2; Published online 1 February 2011
Subject Categories: RNA; development
Keywords: gene expression regulation; iPS cells; miRNA

Introduction

Induced pluripotent stem cells (iPSCs), which exhibit properties similar to embryonic stem (ES) cells, were originally generated by ectopic expression of four transcription factors, Oct4, Sox2, Klf4 and cMyc, in mouse somatic cells (Takahashi and Yamanaka, 2006). In human and mouse somatic cells, besides these factors (Takahashi *et al*, 2007; Lowry *et al*, 2008; Park *et al*, 2008), iPSCs can be generated with an alternative set of four factors, namely Oct4, Nanog, Lin28 and Sox2 (Yu *et al*, 2007). Although cell types from several different tissues are confirmed to be reprogrammable (Meissner *et al*, 2007; Aoi *et al*, 2008; Eminli *et al*, 2008; Hanna *et al*, 2008; Giorgetti *et al*, 2009), a major bottleneck in iPSC derivation and therapeutic use is low reprogramming efficiency, typically from 0.01 to 0.2% (Takahashi and Yamanaka, 2006; Meissner *et al*, 2007; Aoi *et al*, 2008; Nakagawa *et al*, 2008). Although tremendous effort has been focused on screening for small molecules to enhance reprogramming efficiency and on developing new methods for iPSC derivation (Shi *et al*, 2008a, b; Ichida *et al*, 2009; Lyssiotis *et al*, 2009; Maherali and Hochedlinger, 2009; Li *et al*, 2009b), mechanisms underlying reprogramming of primary fibroblasts to an ES cell-like state are still largely unknown.

Several elegant approaches have been employed to improve reprogramming efficiency. Small molecule-based methods have been developed based on observation that treatment of cells with DNA methyltransferase 1 (Dnmt1) inhibitors accelerates reprogramming (Mikkelsen *et al*, 2008). TGF-β inhibition also enables more efficient iPSC induction, as does omission of Sox2 and cMyc (Ichida *et al*, 2009; Maherali and Hochedlinger, 2009). In addition, array analysis shows that partially reprogrammed iPSCs can be created and then pushed to become fully reprogrammed following treatment with factors such as methyl transferase inhibitors (Mikkelsen *et al*, 2008). Genome-wide analysis of promoter binding and induction of gene expression by the four reprogramming factors demonstrates that they bind to similar targets in iPS and mES cells and likely regulate similar sets of genes, and also that targeting of reprogramming factors is altered in partial iPSCs (Sridharan *et al*, 2009). More recently, several groups showed that p53-mediated tumour suppressor pathways may antagonize iPSC induction (Banito *et al*, 2009; Hong *et al*, 2009; Kawamura *et al*, 2009; Utikal *et al*, 2009; Li *et al*, 2009a). Both p53 and its downstream effector p21 are induced during reprogramming, and minimizing expression of both enhances iPSC colony formation. As these proteins are upregulated in most cells expressing the four reprogramming factors, and cMyc reportedly blocks p21 expression (Gartel *et al*, 2001; Seoane *et al*, 2002), it is unclear how ectopic expression of these four factors overcomes the cellular responses to oncogenes/transgenes overexpression and why only a very small population of cells becomes fully reprogrammed.

microRNAs (miRNAs) are 18–24 nucleotide single-stranded RNAs associated with a protein complex called the RNA-induced silencing complex. Small RNAs are usually

*Corresponding author. Program for RNA Biology, Sanford-Burnham Medical Research Institute, 10901 North Torrey Pines Road, La Jolla, CA 92037, USA. Tel.: +1 858 795 5325; Fax: +1 858 795 5328; E-mail: trana@sanfordburnham.org

Received: 11 August 2010; accepted: 22 December 2010; published online: 1 February 2011

generated from non-coding regions of gene transcripts and function to suppress gene expression by translational repression (Ambros, 2004; Bartel, 2004; Rana, 2007; Kim *et al*, 2009a). In recent years, miRNAs have been found to function in many important processes, such as expression of self-renewal genes in human ES (hES) cells (Xu *et al*, 2009), cell cycle control of ES cells (Wang *et al*, 2008), alternative splicing (Makeyev *et al*, 2007) and heart development (Latronico and Condorelli, 2009). Furthermore, it was recently reported that ES cell-specific miRNAs enhanced mouse iPSC derivation and replaced the function of cMyc during reprogramming (Judson *et al*, 2009) and hES-specific miR-302 could alleviate the senescence response due to four factor expression in human fibroblast (Banito *et al*, 2009). However, since these miRNAs are not highly expressed until very late stages of reprogramming, whether miRNAs mediating regulation of gene expression have an important role in iPSC induction remains unknown.

Here, we show that miRNAs function directly in iPSC induction and that interference with the miRNA biogenesis machinery significantly decreases reprogramming efficiency. We also identified three clusters of miRNAs, miR-17∼92, miR-106b∼25 and miR-106a∼363, which are highly induced during early stages of reprogramming. Functional analysis demonstrated that introducing these miRNAs into MEFs enhanced Oct4-GFP+ iPSC colony formation. We also found that Tgfbr2 and p21, both of which inhibit reprogramming, are directly targeted by these miRNAs and that blocking their activity significantly decreased reprogramming efficiency. Overall, we propose that miR-93 and miR-106b are key regulators of reprogramming activity.

Results

Post-transcriptional regulation functions in reprogramming of MEFs to iPSCs

To investigate the role of post-transcriptional gene regulation in iPSC induction, we used lentiviral shRNA vectors targeting mouse Ago2 as well as Dicer and Drosha to stably knock down these factors in primary Oct4-GFP MEFs. Knock-down efficiency of shRNA constructs was verified by both western analysis and RT–qPCR (Figure 1A; Supplementary Figure S1a

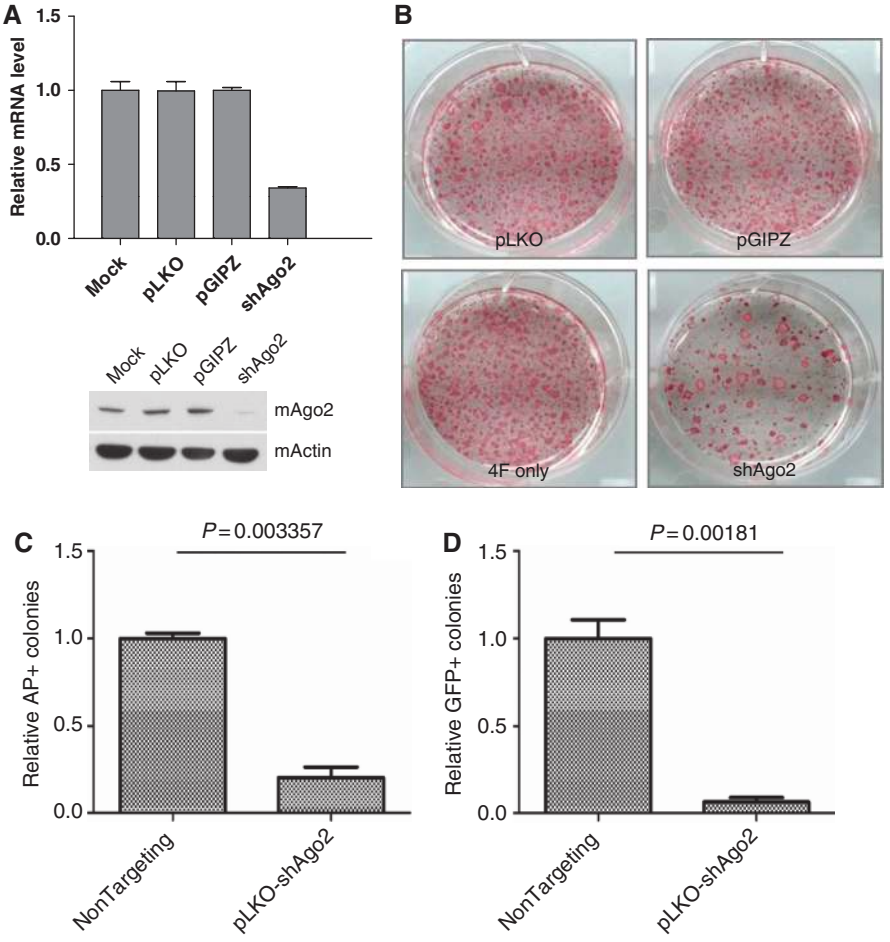

Figure 1 The RNAi machinery functions in mouse iPSC induction. (**A**) Knock-down of mouse RNAi machinery gene Ago2 by shRNAs. MEFs were transduced with lentiviral shRNAs plus 4 μg/μl polybrene, and total RNAs or proteins were harvested at day 3 post-transduction. mRNA and protein levels of targeted genes were analysed by RT–qPCR and western blotting, respectively. pLKO is the empty vector control for the shRNA lentiviral vectors. pGIPZ is a lentiviral vector expressing a non-targeting shRNA. (**B**) Knock-down of Ago2 dramatically decreases iPS induction by 4F. Primary MEFs were transduced with the four reprogramming factors (OSKM (4F)) plus shRNA Ago2. Colonies were stained at day 14 post-transduction for alkaline phosphatase (AP), which is a marker for mES/iPS cells. pLKO and pGIPZ vectors served as negative controls. (**C**) Knock-down of Ago2 decreases iPS induction by OSK. Colonies were stained and quantified for AP at day 21 post-transduction. Error bar represents s.d. of duplicate wells. (**D**) GFP+ colony quantification of iPSC with shAgo2. GFP+ colonies were quantified at day 21 post-transduction. Error bar represents s.d. of duplicate wells.

and b). For each shRNA, we routinely observed ~70–80% mRNA level knock-down, as well as significant decreases in protein levels. We then transduced MEFs with each of these shRNAs separately along with viruses expressing the four OSKM (Oct4, Sox2, Klf4 and cMyc) factors at a volume ratio of 1:1:1:1:1. After 14 days, colonies were fixed and stained for alkaline phosphatase (AP) activity, a widely used ES cell marker. We found that knock-down of either Dicer, Drosha or Ago2 resulted in a dramatic decrease in the number of AP+ colonies compared with pLKO and pGIPZ controls (Figure 1B; Supplementary Figure S1c). We also observed similar results by using OSK (3F) transduction. Both GFP+ and AP+ colony quantification verified that knocking down Ago2 dramatically decrease reprogramming efficiency, while proliferation of transduced fibroblasts were not affected (Figure 1C and D; Supplementary Figure S2).

Despite the decrease in reprogramming efficiency upon Ago2 knock-down, we observed some GFP+ colonies in shAgo2-infected MEFs and further characterization determined that these colonies were positive for shRNA integration and shRNAs were actively expressed (Supplementary Figure S3a and b). These cells also expressed all the tested ES-specific markers and had turned on the endogenous Oct4 locus as well as low expression of p21 and Tgfbr2 (Supplementary Figure S3c–e). Further studies to induce differentiation showed that shAgo2 clones had compromised differentiation capacities as Nanog, one of the self-renewal genes, could not be silenced as efficiently as observed in control ES cells when treated with retinoid acid (Supplementary Figure S3f). Understanding the detailed mechanism of GFP+ colony formation in shAgo2-infected MEFs needs further investigation. Taken together, these data strongly suggest that post-transcriptional regulation, particularly that mediated by miRNAs, functions in the reprogramming process.

miR-17, miR-25, miR-106a and miR-302b clusters are induced during the early stage of reprogramming

Expression of the four reprogramming factors induces numerous changes in gene expression during iPS induction (Mikkelsen *et al*, 2008; Sridharan *et al*, 2009). We hypothesized that some ES cell-specific miRNAs might be induced by these factors to facilitate reprogramming. Based on previously published results (Houbaviy *et al*, 2003; Landgraf *et al*, 2007), we analysed nine miRNA clusters highly expressed in mouse ES (mES) cells (Supplementary Table 1). Two representative miRNAs from each cluster were evaluated using a miR qPCR-based method to quantify expression changes at different reprogramming stages—namely days 0, 4, 8 and 12—following transduction of the OSKM factors. Many ES cell-specific miRNAs, such as the miR-290 and miR-293 clusters, were not induced until day 8 (Supplementary Figure S4), at which stage GFP+ colonies were already detectable. Interestingly, we found that several other clusters, including miR-17~92, miR-106b~25, miR-106a~363 and miR-302b~367, were expressed to varying extents by day 4 of induction (Figure 2A). Among these four clusters, the level of miR-302b~367 in MEFs was the lowest (data not shown). It is noteworthy that of the three clusters highly induced at reprogramming day 4, many shared very similar seed regions (Figure 2B). In general, seed region of a miRNA decides the target specificity, however, recent reports suggest that other mechanisms could also have roles in miRNA targeting (Tay *et al*, 2008; Lal *et al*, 2009; Wang *et al*, 2010). Together, our findings suggest that these miRNAs function in reprogramming and could target similar sets of genes.

We next asked which of the four reprogramming factor(s) induced these miRNAs by transducing MEFs with different combinations of OSKM factors at the same dose and undertaking miR qPCR analysis at day 4 post-infection (Figure 2C). This analysis confirmed that cMyc alone could induce miR-17~92, miR-106b~25 and miR-106a~363 cluster expression, as reported previously (Mendell, 2008). However, in each case, a combination of all four reprogramming factors induced the most abundant expression of miRNA clusters, and that robust expression was correlated with the highest reprogramming efficiency (Figure 2C).

miR-93 and miR-106b enhance iPSC induction and mesenchymal-to-epithelial transition step of reprogramming

As the four identified miRNA clusters contain several miRNAs with similar seed regions, we chose the miR-106b~25 cluster for further analysis because it contains only three miRNAs: miR-25, miR-93 and miR-106b. miR-93 and miR-106b have the identical seed regions, and both were highly induced by the four reprogramming factors (Figure 2A). Besides, miRNAs mimics could be transfected into MEFs with high efficiency and exhibited a half-life of 4 days (Supplementary Figures S7 and S9b). Thus, we reasoned that we might observe more efficient iPSC induction if we ectopically expressed these miRNAs during reprogramming. To test this hypothesis, we directly transfected miRNA mimics into MEFs harbouring Oct4-GFP at days 0 and 5 with vectors expressing either all four factors (4F, OSKM) or only Oct4, Sox2 and Klf4 (OSK) and assayed reprogramming based on GFP expression (Figure 3A). GFP+ colonies were counted on day 11 to evaluate reprogramming efficiency (Figure 3B). Transfection of miR-93 and miR-106b mimics promoted a 4–6-fold increase in the number of GFP+ colonies in both 4F and OSK transduction (Figure 3C and D; Supplementary Figure S22, Supplementary Table 3), confirming that these miRNAs, which are induced during iPSC induction, facilitate MEF reprogramming. Dose/response analysis showed that enhanced reprogramming efficiency occurred at as low as the 5–15 nM range of miRs (Supplementary Figure S5). To confirm that the enhancement by these miRNAs was from induction of bonafide iPS colonies, we further analysed the expression of another marker Nanog in miR-106b-transfected cells. In both 4F and OSK-infected samples, miR-106b transfection consistently increased the relative Nanog expression (Supplementary Figure S6a and b). Immunostaining and followed by Nanog+ colonies quantification further proved that almost every Oct4-GFP+ colony is also Nanog+ at that stage (Supplementary Figure S6c) and miR-106b can enhance formation of both colonies (Supplementary Figure S6d and e). AP staining showed no obvious increase in the number of AP+ colonies in miR mimic transfections (Supplementary Figure S8a), suggesting that miR-93 and miR-106b facilitate maturation of iPS colonies. This idea was supported by our observation of the OSK system, in which many GFP+ colonies were apparent at day 15 post-OSK transduction in miR mimic-transfected cells, while control wells did not exhibit any mature iPS colonies at this stage (data not shown).

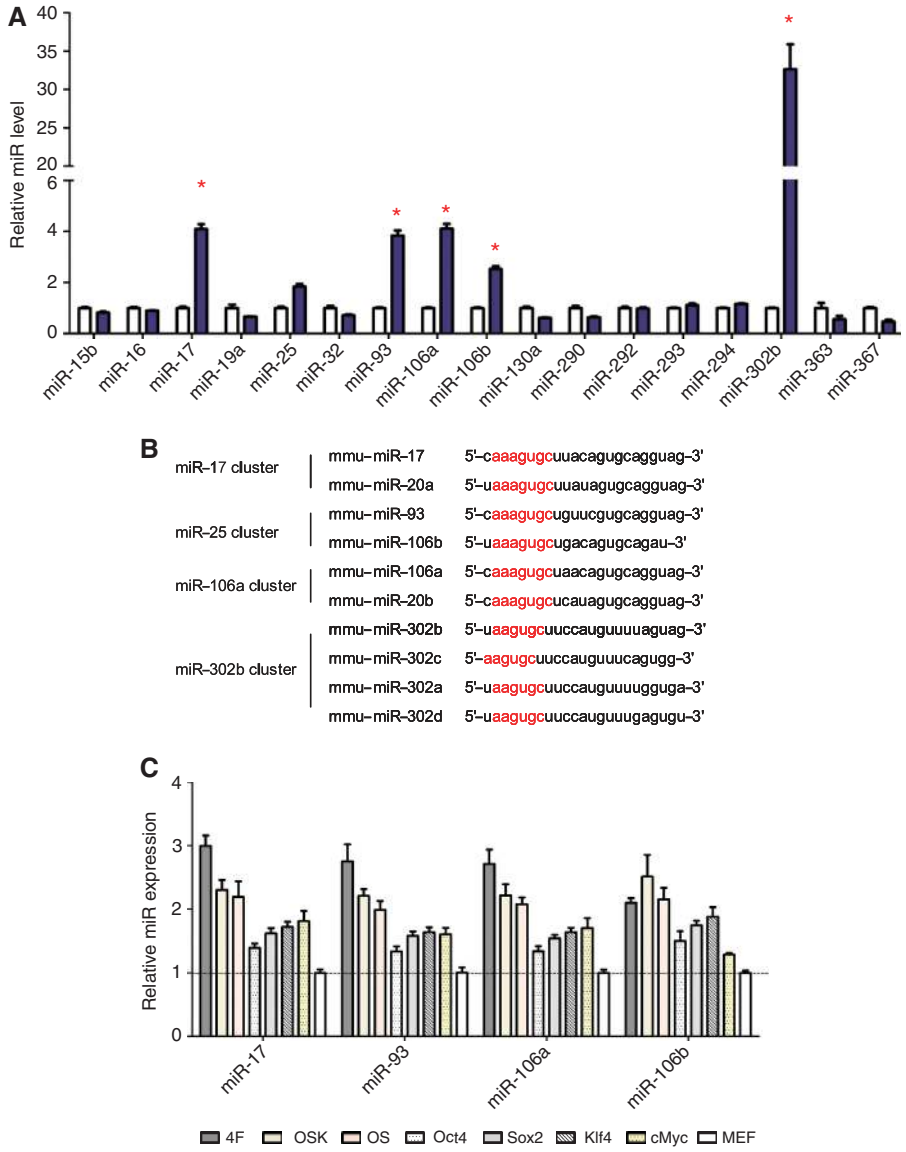

Figure 2 miR-17, miR-25, miR-106a and miR-302b clusters are induced during early stages of reprogramming. (**A**) Induction of 10 miRNA clusters in the early stages after transduction with the four reprogramming factors. miR RT–qPCR was used to quantify expression levels of representative miRNAs from clusters highly expressed in ES cells. Total RNAs from day 0 MEFs and from MEFs transduced with reprogramming factors at day 4 post-infection were analysed. Blue bars: day 4 MEFs; white bars: day 0 MEFs. Asterisks indicate induced miRNAs. (**B**) Seed region comparison of different miR clusters induced at day 4 post-reprogramming factor transduction. Red indicates similar seed regions. (**C**) Representative miRNAs can be induced with different combinations of reprogramming factors. miRNA expression was quantified at 4 days post-transduction.

To confirm that these miRNAs have an important role in iPSC induction, we used miR inhibitors (Hutvagner *et al*, 2004; Meister *et al*, 2004; Vermeulen *et al*, 2007) to knock down targeted miRNAs during the reprogramming process. All of the miR inhibitors could efficiently decrease target miR expression and their transfection did not affect proliferation (Supplementary Figure S9a and c). Consistent with miR mimic experiments, miR-93 and miR-106b knock-down promoted a dramatic decrease in the number of GFP+ colonies (Figure 3E). It is also noteworthy that although the miR-25 mimic did not enhance MEF iPS induction, knocking down this miRNA decreased reprogramming efficiency by ~40% (Figure 3E). These results suggest that miR-25 could also function during reprogramming.

Recent reports have identified that during the initial stage of reprogramming, a mesenchymal-to-epithelial transition (MET) is required (Li *et al*, 2010; Samavarchi-Tehrani *et al*, 2010). E-Cadherin is one of the most important genes for MET process and we used it as the marker to determine whether miR-106b could facilitate this step of iPSC generation. We detected a significant increase of E-Cadherin expression in both 4F and OSK-infected samples (Figure 3F and G). In addition, knocking down of miR-106b also dramatically decreased the induction of E-Cadherin expression (Figure 3H). Overall, these data indicate that miR-93 and miR-106 promote reprogramming of MEFs to iPSCs and modulate MET transition in the initiation step of reprogramming.

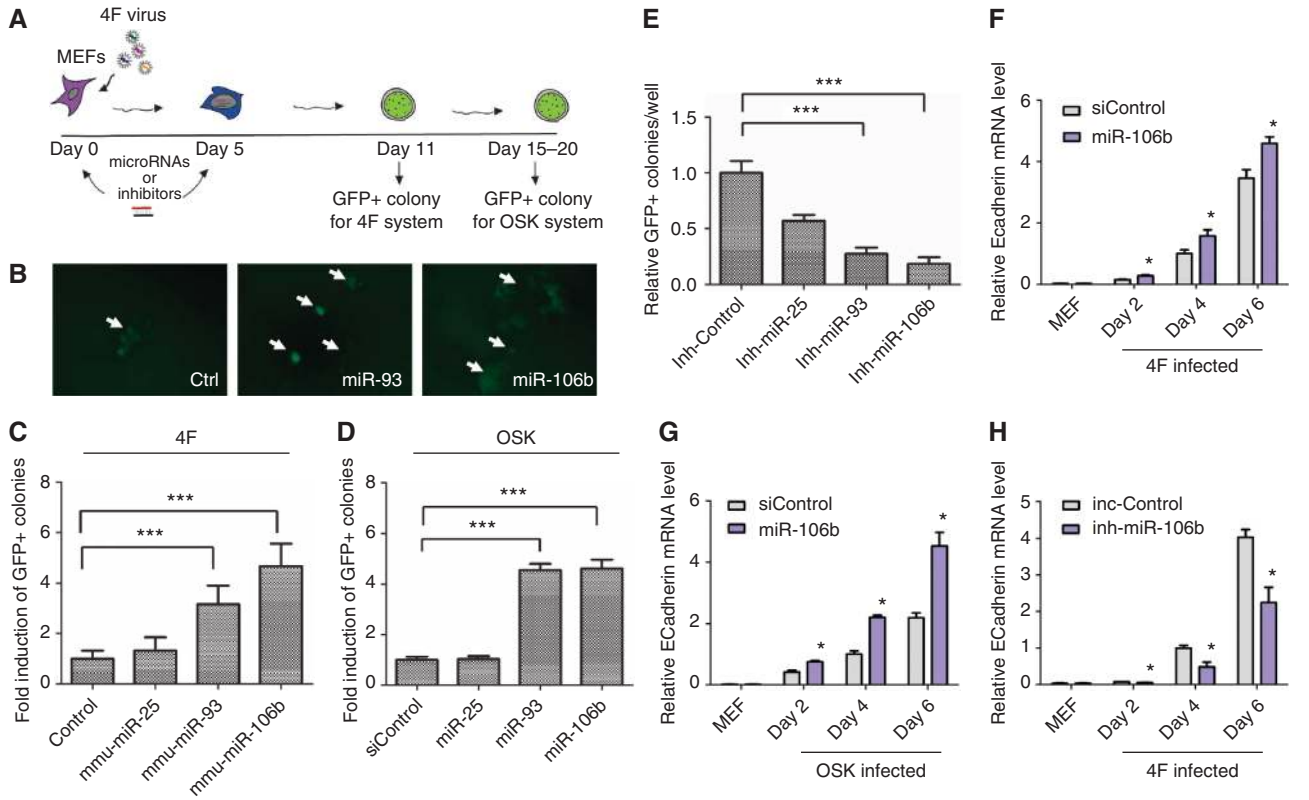

Figure 3 miR-93 and miR-106b greatly enhance iPS induction. (**A**) Reprogramming assay timeline. miRNA mimics or inhibitors were transfected at a final concentration of 50 nM on days 0 and 5 of reprogramming. GFP+ colonies were quantified at day 11 for 4F induction and days 15–20 for OSK induction. (**B**) Representative images of GFP+ colonies from reprogrammed Oct4-GFP MEFs transfected with miRNA mimics. Arrows indicate GFP+ colonies. (**C**) miR-93 and miR-106b mimics enhance iPS induction with 4F induction. Oct4-GFP MEFs were transfected with 50 nM of the indicated miRNAs at days 0 and 5 of reprogramming. GFP+ colonies were quantified at day 11 post-transduction. Fold induction and error bars were calculated from three independent experiments in triplicate wells. ***$P<0.0001$. (**D**) The enhancing effect of miR-93 and miR-106b is observed using the OSK system. miRNA mimics were transfected as in 4F experiments. GFP+ colonies were quantified on days 15–20. Error bars represent s.d. of three independent experiments in triplicate wells. ***$P<0.0001$. (**E**) miR-93 and miR-106b inhibitors dramatically decrease reprogramming efficiency. miRNA inhibitors were transfected at a final concentration of 50 nM. The experimental timeline was the same as in miR mimic transfections. Error bars represent s.d. of three independent experiments in triplicate wells. ***$P<0.0001$. (**F**) miR-106b promotes the MET transition during 4F-mediated reprogramming. miR-106b mimic was transfected into MEFs and cells were harvested at different time points to analyze E-Cadherin expression. Fold induction of ECad was normalized to day 4 samples after 4F infection. Error bars represent s.d. of three independent experiments. *$P<0.001$. (**G**) miR-106b promotes the MET transition in OSK-infected cells. The experimental procedures were the same as in (**F**). Fold induction of ECad was normalized to day 4 samples after OSK infection. Error bars represent s.d. of three independent experiments. *$P<0.001$. (**H**) Inhibition of miR-106b decreases induction of MET process. The experimental procedures were the same as in (**F**), except anti-miR oligos were transfected instead of miR mimics. Fold induction of ECad was normalized to day 4 samples after 4F infection. Error bars represent s.d. of three independent experiments. *$P<0.001$.

miRNA-derived clones are fully pluripotent

Next, we asked whether induced cells reached a fully pluripotent state. To answer this question, several iPS clones for each miRNA as well as miR controls were derived and analysed for expression of pluripotency markers. All clones were GFP+ indicative of reactivated Oct4 expression (Figure 4A). Immunostaining confirmed that Nanog and SSEA1 were also activated in all clones (Figure 4B). RT–qPCR for other mES markers such as ERas, ECatI and endogeneous Oct4 showed similar results (Figure 4C). Whole genome mRNA expression profiling also indicated that derived clones exhibited a gene expression pattern more similar to mES cells than MEFs (Supplementary Figure S10a). Promoter methylation of endogenous Nanog loci was also analysed, and all tested clones showed demethylated promoters, as is observed in mES cells (Blelloch *et al*, 2006) (Supplementary Figure S10b).

To investigate whether derived clones exhibit the full differentiation capacity of mES cells, we evaluated embryoid body (EB) formation. All derived clones showed efficient EB formation, and EBs showed positive staining for lineage markers such as β-tubulin III (ectoderm), AFP (endoderm) and α-actinin (mesoderm) (Figure 4D). Beating EBs were also derived from these cells (Supplementary Video 1), indicating that functional cardiomyocytes can be derived from these miR-iPSC clones (Supplementary Videos 2 and 3). When these miR-iPSCs were injected into athymus nude mice, teratomas were readily derived in 3–4 weeks (Figure 4E). Finally, as a more stringent test, we injected miR-derived iPSC clones into albino/black B6 blastocysts and generated chimera mice (Figure 4F). Furthermore, these cells could contribute to the genital ridge of derived E13.5 embryos (Supplementary Figure S11). Taken together, these results indicate that the enhancing effects of miR-93 and miR-106b on reprogramming do not alter differentiation capacity of induced pluripotent cells and that those derived clones can differentiate into all three germ lines.

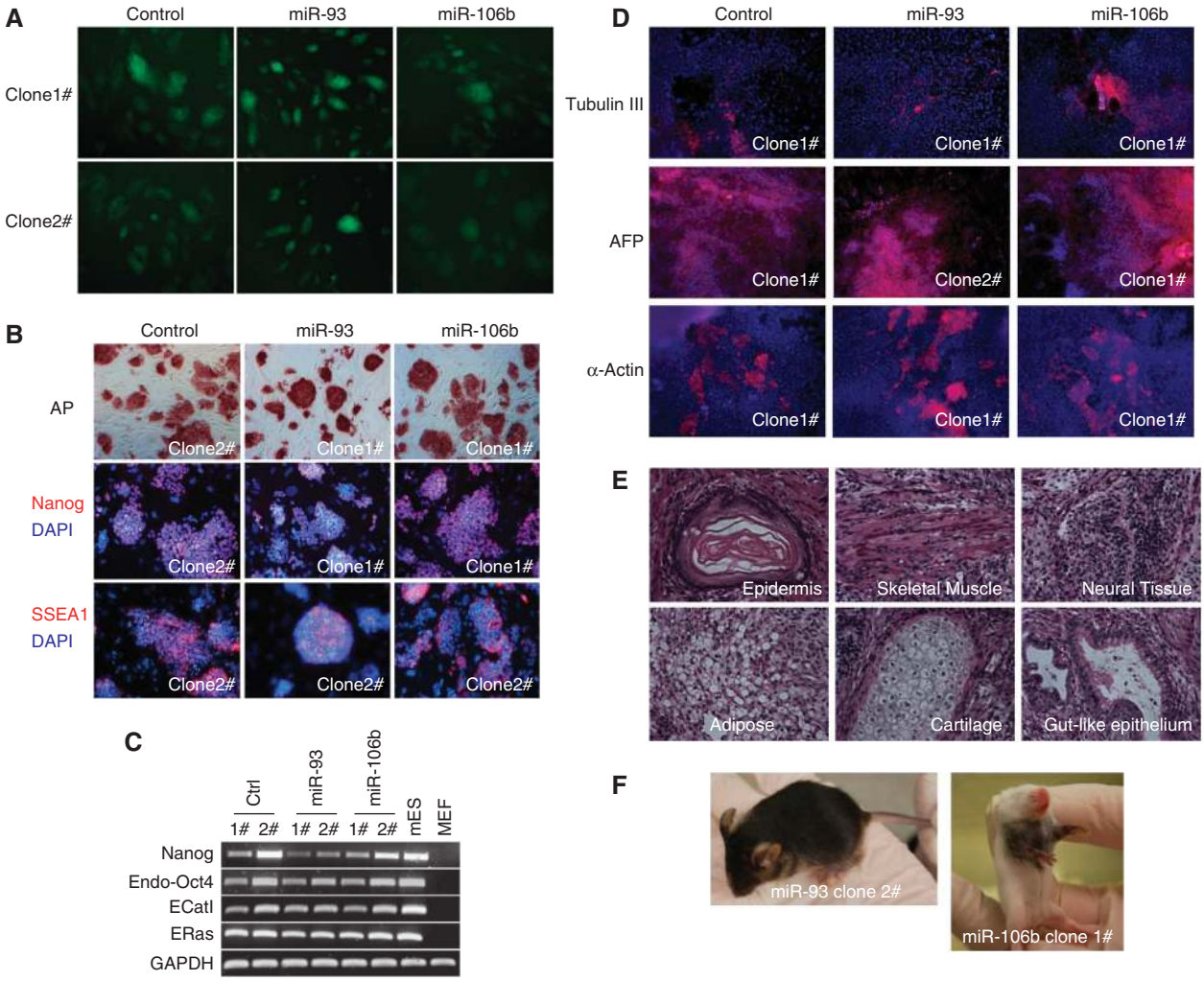

Figure 4 Characterization of iPS clones derived from miR mimic experiments. (**A**) Derived clones activate endogenous Oct4-GFP expression. Colonies were picked starting at day 12 post-OSKM transduction with miRNA mimics and maintained on irradiated MEF feeder plates. Green fluorescence is GFP signal from the endogenous *pou5f1* locus. (**B**) Clones shown in (**A**) are positive for alkaline phosphatase staining and immunostaining of ES-specific markers based on Nanog and SSEA1 staining. Hoechst 33342 was used for nuclear staining. (**C**) RT–PCR of endogenous ES markers. Total RNAs were isolated from iPS cell lines at day 3 post-passage. ES cell-specific markers such as ERas, ECatI, Nanog and endogenous Oct4 expression were analysed by RT–PCR. (**D**) Cells from all three germ layers can be obtained in embryoid body (EB) assays using derived iPS clones. iPS cells were cultured for EB formation at ~4000 cells/20 μl drop for 3 days, and EBs were then reseeded onto gelatin-coated plates for further culture until day 12–14, when beating cardiomyocytes were observed (Supplementary Video 1). Cells were immunostained with different lineage markers: β-tubulin III, ectoderm marker; AFP, endoderm marker; α-actinin, mesoderm marker. (**E**) Teratomas form from injected iPS cells. In total, 1.5 million cells were injected into each mouse, and tumours were harvested 3–4 weeks after injection for paraffin embedding and H&E staining. Structures representing different lineages are labeled. Representative pictures are from miR-106b clone 1#. (**F**) Derived clones can be used to generate chimeric mice. iPS cells were injected into blastocysts from albino or black C57B6 mice (NCI) and the contribution of iPSCs can be seen with agouti or black coat colour.

miR-93 and miR-106b target Tgfbr2 and p21

To further understand the mechanism underlying miR-93 and miR-106b enhancement of reprogramming efficiency, we investigated cellular targets of these miRNAs. We chose miR-93 for analysis since it shares the same seed region as miR-106b. miR-93 mimics were transfected into MEFs, and total RNAs were harvested at day 2 for mRNA expression profile analysis (Supplementary Table 4). That analysis identified potential functional targets of miR-93 that we compared with published expression profiles of MEFs and iPSCs (Sridharan *et al*, 2009). We found that genes significantly decreased upon miR-93 transfection showed a 3-fold enrichment of genes, which are lowly expressed in iPSCs (Supplementary Figure S13a), while genes which were increased upon miR-93 transfection did not show such enrichment. In addition, we undertook pathway ontology analysis of the expression profile of miR-93-transfected MEFs (data not shown). Interestingly, two important pathways for iPS induction were regulated by miR-93: TGF-β signaling and G1/S transition pathways.

For TGF-β signaling, Tgfbr2 is among one of the most significantly decreased genes upon miR-93 transfection. Tgfbr2 is a constitutively active receptor kinase that has a critical role in TGF-β signaling, and recent small molecule screens indicate that inhibitors of its heterodimeric partner Tgfbr1 enhance iPSC induction (Ichida *et al*, 2009; Maherali and Hochedlinger, 2009). miRNA target site prediction suggested that there were two conserved targeting sites for

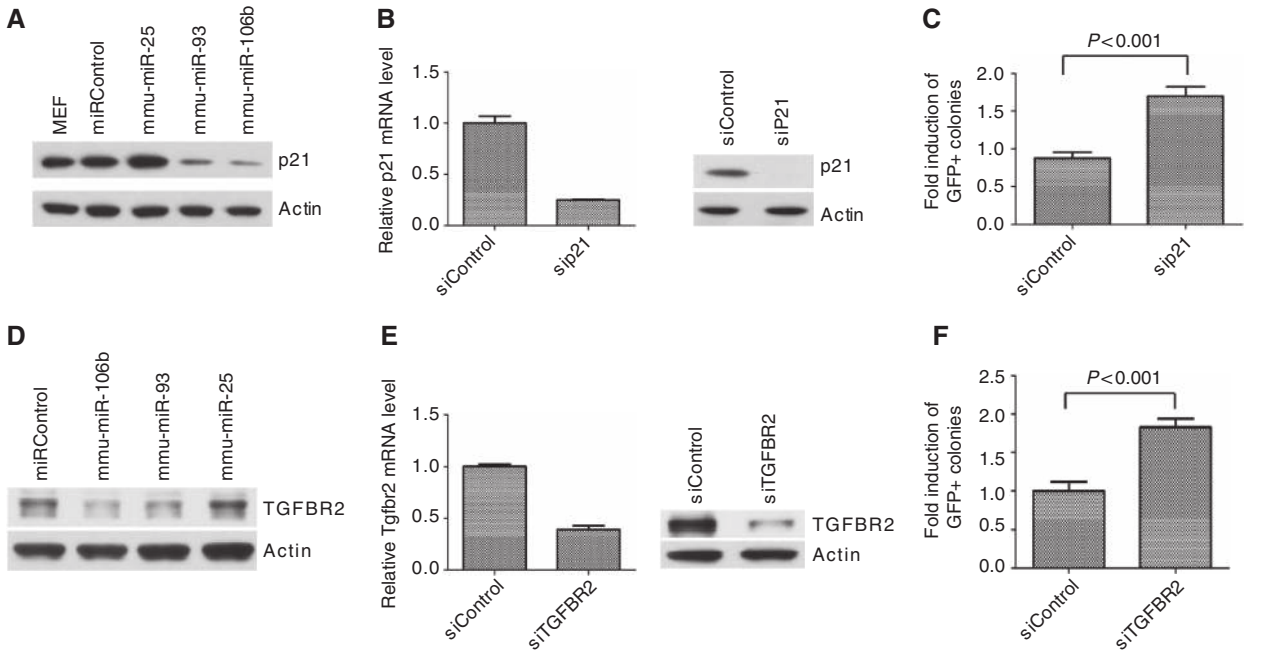

Figure 5 miR-93 and miR-106b directly target mouse p21 and Tgfbr2. (**A**) miR-93 and miR-106b transfection decreases p21 protein levels. Oct4-GFP MEFs were transfected with 50 nM miR mimics and harvested 48 h after transfection for western analysis. Actin was used as the loading control. (**B**) p21 is knocked down efficiently by siRNA. p21 siRNA- and control-transfected MEFs were harvested at 48 h and RT–qPCR, and western blotting was undertaken to verify p21 expression. p21 mRNAs were normalized to GAPDH. (**C**) Knock-down of p21 by siRNA enhances iPSC induction. MEFs were infected with 4F virus, and siRNAs were transfected following the same timeline as miRNAs mimic transfection. GFP+ colonies were quantified at day 11. Error bars represent three independent experiments in triplicate wells. (**D**) miR-93 and miR-106b transfection decreases TGFBR2 expression. Transfected cells were harvested at 48 h for western blotting. (**E**) Tgfbr2 is knocked down by siRNAs. Relative Tgfbr2 mRNA levels were normalized to those of GAPDH. (**F**) Knock-down of Tgfbr2 by siRNAs enhances iPSC induction. Error bars represent four independent experiments in triplicate wells.

miR-93 and its family miRNAs in its 3′UTR. Therefore, we choose it as the candidate target for further investigation.

Regarding the G1/S transition, we choose p21 as the potential target because recent results in human solid tumour samples (breast, colon, kidney, gastric and lung) and gastric cancer cell lines indicate that the miR-106b∼25 cluster can target cell cycle regulators, such as the CDK inhibitors p21 and p57 (Ivanovska *et al*, 2008; Kim *et al*, 2009b) and that human and mouse p21 share a conserved miR-93/106b target site in the 3′UTR. Furthermore, mES cell-specific miRNA clusters, such as miR-290 and miR-293, reportedly target negative regulators of the G1/S transition, including p21 (Wang *et al*, 2008). miR-290 and miR-293 cluster miRNAs also share very similar seed regions with miR-93 and miR-106b (unpublished observations). p21 is also greatly induced by OSKM factors during early stages of iPSC induction (Kawamura *et al*, 2009), an upregulation that we confirmed in MEFs (Supplementary Figure S12a). Detailed analysis revealed that p21 induction is primarily due to Klf4 and cMyc misexpression, as a combination of Oct4 and Sox2 only did not significantly alter p21 protein levels (Supplementary Figure S12a).

To determine whether mouse Tgfbr2 and p21 are targeted by miR-93 and miR-106b, miR mimics were transfected into MEFs (Supplementary Table 5) and total cell lysates were analysed by western blotting 48 h later. Indeed, miR-93 and miR-106b expression efficiently decreased both Tgfbr2 and p21 protein levels (Figure 5A and D) and p21 mRNA levels were decreased by ∼25–30% while Tgfbr2 was decreased by ∼60–70% (Supplementary Figure S14a and b). These levels of suppression were further confirmed in 4F and OSK-infected MEFs (Supplementary Figures S15 and S16). To determine whether p21 is a direct target of miR-93 and miR-106b, we constructed a luciferase reporter with p21 3′UTR sequence inserted downstream of the firefly luciferase coding sequence. We observed consistent ∼40% repression of luciferase activity following transfection of miR-93 and miR-106b mimics into co-transfected Hela cells, a repression lost when mutations were introduced into the seed region of conserved p21 3′UTR target sites (Supplementary Figure S17a and b). For Tgfbr2, luciferase assay also showed ∼50% decrease of GL activity while miR-93 mutant did not have such effect (Supplementary Figure S18a and b).

Cell cycle arrest promoted by p21 may inhibit epigenetic modifications required for reprogramming, as those modifications occur more readily in proliferating cells. To determine whether p21 expression compromises iPS, HA-tagged p21 cDNA was cloned into the pMX retroviral backbone and overexpressed in MEF cells. When HA-p21 virus was introduced into MEFs together with the four OSKM factors, an almost complete inhibition of iPS induction was observed, based on both AP staining and Oct4-GFP-positive colony formation (Supplementary Figure S19a). Similar results were obtained when the three OSK factors were used for reprogramming (Supplementary Figure S19b).

As our analysis indicated that miR-93 and miR-106b efficiently repress both Tgfbr2 and p21 expression, we asked whether Tgfbr2 and p21 activity antagonizes reprogramming. To do so, we transfected Tgfbr2 or p21 siRNAs into MEFs using the same experimental timeline employed

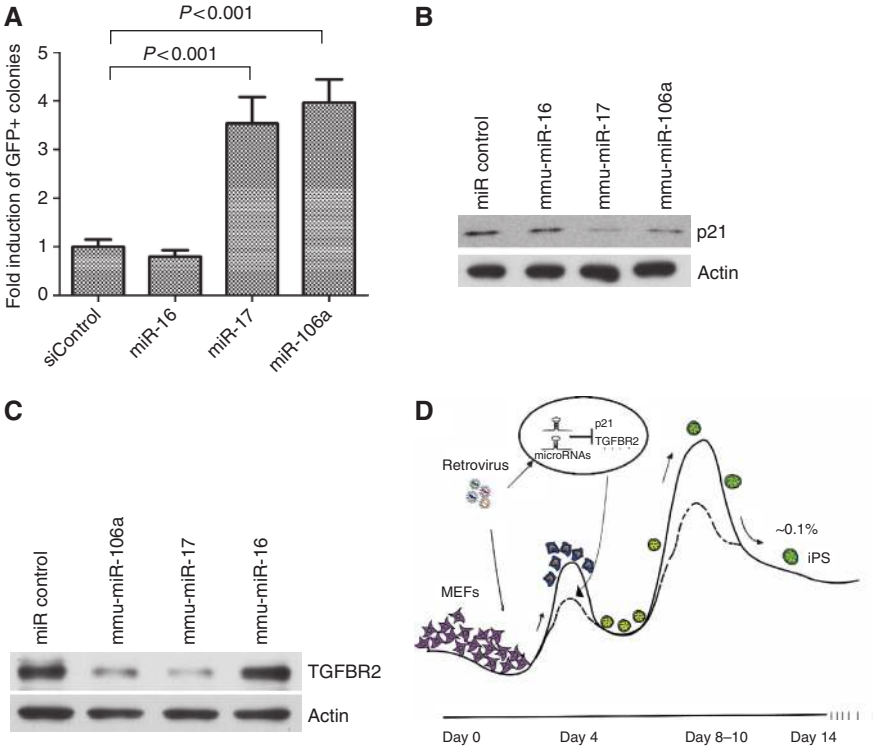

Figure 6 Reprogramming is enhanced by other family miRNAs. (**A**) miR-17 and miR-106a can also enhance reprogramming efficiency. miR-17 and miR-106a mimics were transfected into MEFs at a final concentration of 50 nM. GFP + colonies were quantified at day 11 post-transduction. Error bars represent three independent experiments in triplicate wells. (**B**) miR-17 and miR-106a also target p21. p21 western blotting was performed 2 days after transfection of miRNA mimics into MEFs. (**C**) miR-17 and miR-106a target TGFBR2 expression. miRNA mimics were transfected into MEFs at 50 nM final concentration. Western blotting was performed 2 days post-transfection. (**D**) Model for the role for miRNAs during iPS induction. Several miRNAs, including miR-17, miR-25 and miR-106a clusters, are induced during early stages of reprogramming. These miRNAs facilitate full reprogramming by targeting factors that antagonize the process, such as p21 and other unidentified proteins. Up and down represent the potential different stages and barriers during reprogramming process and dashed line indicates that barriers for reprogramming which are lowered upon miRNAs induction in reprogrammed cells.

with miRNA mimics. Western blotting and RT–qPCR confirmed that both protein and mRNA levels, respectively, were efficiently knocked down by siRNAs without virus transduction (Figure 5B and E). MEF reprogramming was then initiated by OSKM transduction, and Oct4-GFP + colonies were quantified at day 11 post-transduction. We observed a ~2-fold induction in colony number for each gene (Figure 5C and F). TGF-β receptor II (TGFBR2) was also overexpressed in MEFs, and iPS enhancement by miR-106b was compromised under such condition (Supplementary Figure S20). Altogether, our data identify that Tgfbr2 and p21 are the direct target of miR-93 and miR-106b and down regulation of these genes can enhance the reprogramming process.

Additional upregulated miRNAs enhance iPSC induction

As noted, we identified three miRNA clusters induced by reprogramming factors, and several miRNAs within these clusters have the same seed regions, suggesting that they target similar mRNAs (Figure 2). To investigate whether other miRNAs that share the same seed region with miR-93 and miR-106b also enhance iPSC induction, miRNA mimics of miR-17 and miR-106a were tested using an experimental procedure similar to that described above for miR-93 mimic treatment and iPSC induction. These miRNAs enhanced reprogramming in a manner similar to that seen with the miR-106b~25 clusters (Figure 6A), and transfection of these miRs resulted in decreased TGFBR2 and p21 protein levels (Figure 6B and C) as well as Tgfbr2 mRNA (Supplementary Figure S21). Together, this evidence suggests that induction of miR-17~92, miR-106b~25 and miR-106a~363 clusters is important for proper reprogramming and that upregulation of these miRNAs lowers reprogramming barriers to the iPSC generation process (Figure 6D).

Discussion

Since the discovery that MEFs can be reprogrammed to iPSCs, much effort has been directed toward understanding fundamental mechanisms underlying this process. Our results show for the first time that post-transcriptional gene regulation occurs during reprogramming and that interference with the RNAi machinery can significantly alter reprogramming efficiency. We identified three miRNAs clusters significantly upregulated by the four factors used to induce iPSCs and found that miRNAs in those clusters likely target two important reprogramming pathways: TGF-β signaling and cell cycle control. While these experiments were in progress, several investigators also reported that the p53 pathway, which includes downstream tumour suppressors such as p21, is a major barrier to iPSC induction (Banito *et al*, 2009; Hong *et al*, 2009; Kawamura *et al*, 2009; Utikal *et al*, 2009; Li *et al*, 2009a). Much evidence indicates that ectopic

expression of the four factors (OSKM) readily upregulates p53 and initiates cellular 'defense programs', such as cell cycle arrest, apoptosis or DNA damage responses. These responses likely underlie low reprogramming efficiency, which we observe to be ~0.1%. However, these data do not explain how successfully reprogrammed cells overcome these barriers to become iPSCs. Our data suggest that cells do so in part by inducing expression of miRNAs that target pathways that antagonize successful reprogramming. By modulating miRNA levels in primary fibroblasts, we were able to achieve a significant increase in reprogramming efficiency.

TGF-β signaling is an important pathway that functions in processes as diverse as gastrulation, organ-specific morphogenesis and tissue homeostasis (Moustakas and Heldin, 2009). The current model of canonical TGF-β transduction indicates that TGF-β ligand binds the TGFBR2, which then heterodimerizes with TGF-β receptor I (TGFBR1) to transduce signals through receptor-associated Smads (Kahlem and Newfeld, 2009). TGF-β signaling reportedly functions in both hES and mES cell self-renewal, and FGF2, a widely used growth factor for ES cell culture, induces TGF-β ligand expression and suppresses BMP-like activities (Greber *et al*, 2007; Ogawa *et al*, 2007). Blocking TGFBRI family kinases by chemical inhibitors compromises ES cell self-renewal (Ogawa *et al*, 2007). These findings are particularly significant for iPSC induction, because those inhibitors seem to have completely different roles during reprogramming. Recent chemical screening has shown that small molecules inhibitors of the TGFBR1 actually enhance iPSC induction and can replace the requirement for Sox2 by inducing Nanog expression (Ichida *et al*, 2009). Moreover, treating reprogramming cells with TGF-β ligands has a negative effect on iPSC induction (Maherali and Hochedlinger, 2009). Therefore, although TGF-β signaling is important for ES cell self-renewal, it is a barrier for reprogramming. Our results determined that, in addition to TGFBR1, activity of the constitutively active kinase TGFBR2 also antagonizes reprogramming. Here, for the first time, we demonstrate that miR-93 and its family members directly target TGFBR2 to modulate its' signaling and reprogramming.

p21, a protein of only 165 amino acids, functions as a tumour suppressor by mediating p53-dependent G1 growth arrest and promoting differentiation and cellular senescence (Abbas and Dutta, 2009). Our data (Supplementary Figure S11) and that of others (Kawamura *et al*, 2009) demonstrate that p21 expression is upregulated when the four factors (OSKM) are introduced into MEFs and that this upregulation antagonizes reprogramming, as p21 overexpression almost completely blocked iPSC induction (Supplementary Figure S16). p21 induction in reprogramming cells could be dependent or independent of p53, as the Klf4 reprogramming factor reportedly binds to the p21 promoter and increases p21 transcription (Abbas and Dutta, 2009). This finding raises an interesting question regarding the function of the four reprogramming factors, as the same transcription factor can both promote and antagonize iPSC induction. In fact, we cannot currently rule out the possibility that a certain level of p21 induction benefits the reprogramming process. Besides its well-known role in p53-dependent cell cycle arrest, p21 also reportedly has an oncogenic activity by protecting cells from apoptosis, a function unrelated to its usual role in cell cycle control (Abbas and Dutta, 2009). A potential benefit for p21 in reprogramming may depend on its ability to regulate gene expression through protein–protein interactions (Abbas and Dutta, 2009). For example, p21 directly binds to several proteins regulating apoptosis, such as caspases 8 and 10 and procaspase 3. It also suppresses pro-apoptotic activity of Myc by associating with the Myc N-terminus to block Myc-Max heterodimerization (Abbas and Dutta, 2009). Indeed, when Myc itself is overexpressed in MEFs, a significant increase in cell death is observed in cell culture, while in four-factor transduced cells, cell death is minimal compared with Myc-only samples (data not shown). Therefore, p21 induction may not only serve as a barrier to reprogramming but may maintain levels of p21 necessary to reduce apoptosis and thus increase reprogramming efficiency. Our data serve as partial evidence to support this hypothesis, as miR-93 and miR-106b treatment had greater enhancing effects on reprogramming than did p21 siRNA transfection (Figures 3C, 5A and C). It is also possible that this effect is due to targeting of multiple proteins such as TGFBR2 in addition to p21 by these miRNAs.

Finally, as the miR clusters identified here, such as miR-17~92, miR-106b~25 and miR-106a~363, are induced during iPS induction and are conserved between mouse and humans, the enhancing effects of miR-93 and miR-106b may apply to human reprogramming. Further studies should focus on the activity of these miRNAs in human cells and in various disease models.

Materials and methods

Cell culture, vectors and virus transduction

Oct4-GFP MEFs were derived from mice carrying an IRES–EGFP fusion cassette downstream of the stop codon of *pou5f1* (Jackson Lab, Stock#008214) at E13.5. MEFs were cultured in DMEM (Invitrogen, 11995-065) with 10% FBS (Invitrogen) plus glutamine and NEAA. Only MEFs at passage of 0–4 were used for iPS induction. pMX-Oct4, Sox2, Klf4 and cMyc were purchased from Addgene. pMX-HA-p21 was generated by inserting N-terminally tagged-p21 into the pMX *Eco*RI site. pLKO-shRNA clones were purchased from Open Biosystems. To generate retrovirus, PLAT-E cells were seeded in 10 cm plates, and 9 μg of each factor was transfected the next day using Lipofectamine (Invitrogen, 18324-012) and PLUS (Invitrogen, 11514-015). Viruses were harvested and combined 2 days later. For iPS induction, MEFs were seeded in 12-well plates and transduced with 'four factor' virus the next day with 4 μg/ml polybrene. One day later, the medium was changed to fresh MEF medium, and 3 days later it was changed to mES culture medium supplemented with LIF (Millipore, ESG1107). GFP+ colonies were picked at day 14 post-transduction, and expanded clones were cultured in DMEM with 15% FBS (Hyclone) plus LIF, thioglycerol, glutamine and NEAA. Irradiated CF1 MEFs served as feeder layers to culture mES cells and derived iPS clones. To generate shRNA lentivirus, shRNA lentiviral vectors were co-transfected into 293FT cells together with the pPACK-H1 packaging system (SBI, LV500A-1). Lentiviruses were harvested at day 2 after transfection and centrifuged at 4000 r.p.m. for 5 min at room temperature. shRNA virus was added together with four factor virus at a volume ratio of 1:1:1:1:1.

miRNA and siRNA transfection of MEFs

miRNA mimics and inhibitory siRNAs were purchased from Dharmacon. To transfect MEFs, miRNA mimics or inhibitors were diluted in Opti-MEM (Invitrogen, 11058-021) to the desired final concentration. Lipofectamine 2000 (Invitrogen, 11668-019) was added to the mix at 2 μl/well in 12-well plates, which were incubated for 20 min at room temperature. For 12-well transfections, 80 μl of the miR mixture was added to each well with 320 μl of Opti-MEM. Three hours later, 0.8 ml of the virus mixture (for iPS) or

fresh medium was added to each well and the medium was changed to fresh MEF medium the next day.

Western blotting

Total cell lysates were prepared by incubating cells in MPER buffer (PIERCE, 78503) on ice for 20 min, and then cleared by centrifugation at 13 000 r.p.m. for 10 min. An equal volume of lysates was loaded onto 10% SDS–PAGE gels, and proteins were transferred onto PVDF membranes (Bio-Rad, 1620177) using the semi-dry system (Bio-Rad). Membranes were blocked with 5% milk in TBST for at least 1 h at room temperature or overnight at 4°C. Antibodies used include anti-p21 (BD, 556430), anti-mNanog (R&D, AF2729), anti-h/mSSEA1 (R&D, MAB2156), anti-HA (Roche, 11867423001), anti-mAgo2 (Wako, 01422023), anti-Dicer (Abcam, ab13502), anti-Drosha (Abcam, ab12286), anti-Actin (Thermo, MS1295P0), anti-AFP (Abcam, ab7751), anti-β III tubulin (R&D systems, MAB1368), anti-TGBR2 (Cell signaling, 3713s) and anti-α actinin (Sigma, A7811).

mRNA and miRNA qPCR

Total RNAs were extracted using Trizol (Invitrogen). After extraction, 1 μg total RNA was used for RT using Superscript II (Invitrogen). qPCR was performed using a Roche LightCycler480 II and the Sybr green mixture from Abgene (Ab-4166). Mouse Ago2, Dicer, Drosha, Gapdh and p21 primers are listed in Supplementary Table 2. Other primers were previously described (Takahashi and Yamanaka, 2006). For miRNA quantitative analysis, total RNA was extracted using the method above. After extraction, 1.5–3 μg of total RNA was used for miRNA reverse transcription using QuantiMir kit following the manufacturer's protocol (SBI, RA420A-1). RT products then were used for qPCR using the mature miRNA sequence as a forward primer together with the universal primer provided with the kit.

Immunostaining

Cells were washed twice with PBS and fixed with 4% paraformaldehyde at room temperature for 20 min. Fixed cells were permeabilized with 0.1% Triton X-100 for 5 min. Cells were then blocked in 5% BSA in PBS containing 0.1% Triton X-100 for 1 h at room temperature. Primary antibody was diluted from 1:100 to 1:400 in 2.5% BSA PBS containing 0.1% Triton X-100, according to the manufacturer's suggestion. Cells were stained with primary antibody for 1 h and then washed three times with PBS. Secondary antibody was diluted 1:400 and cells were stained for 45 min at room temperature.

EB formation and differentiation assay

iPSCs were trypsinized into a single cell suspension and the hanging drop method was used to generate EBs. For each drop, 4000 iPSCs in 20 μl EB differentiation medium were used. EBs were cultured in hanging drops for 3 days before being reseeded onto gelatin-coated plates. After reseeding, cells were further cultured until day 14 when beating areas could be identified.

Promoter methylation analysis

CpG methylation of the Nanog and Pou5f1 promoters was analysed following procedures described elsewhere (Takahashi and Yamanaka, 2006). Briefly, genomic DNA of derived clones was extracted using a Qiagen kit. In total, 1 μg DNA was then used for genome modification analysis following the manufacturer's protocol (EZ DNA Methylation—Direct Kit, Zymo Research, D5020). After modification, PCR of selected regions was performed, and the products were cloned into pCR2.1-TOPO (Invitrogen). Ten clones were sequenced for each gene.

Teratoma formation and chimera generation

To generate teratomas, iPSCs were trypsinized and resuspended at a concentration of 1×10^7 cells/ml. Athymus nude mice were first anesthetized with Avertin, and then ~150 μl of the cell suspension was injected into each mouse. Mice were checked for tumours every week for 3–4 weeks. Tumours were harvested and fixed in zinc formalin solution for 24 h at room temperature before paraffin embedding and H&E staining. To test the capacity of derived iPSC clones to contribute to chimeras, iPSCs were injected into C57BL/6J-Tyr$^{(C-2J)/J}$ (albino) blastocysts. Generally, each blastocyst received 12–18 iPSCs. ICR recipient females were used for embryo transfer. The donor iPSC cells are in either agouti or black colour.

mRNA microarray analysis

miR-93 and siControl were transfected into MEFs and total RNAs were harvested at 48 h post-transfection. mRNA microarray was carried out by Microarray facility in Sanford-Burnham Institute. Gene lists for both potential functional targets (fold change >2, $P<0.05$) and total targets (fold change $>25\%$, $P<0.05$) were generated by filtering through volcano maps. Gene lists were then used for ontology analysis using GeneGo software following guidelines from the company.

Dual luciferase assay

3′UTR of both p21 and Tgfbr2 were cloned into *Xba*I site of pGL3 control vectors. For each well of 12-well plates, 200 ng of resulted vectors and 50 ng of pRL-TK (renilla luciferase) were transfected into 1×10^5 Hela cells which were seeded 1 day before the transfection. In total, 50 nM of miRNAs were used for each treatment and cell lysates were harvested at day 2 post-transfection. In total, 20 μl of lysates were then used for dual luciferase assay following the manufacturer's protocol (Dual-Luciferase® Reporter Assay System Promega, E1910).

Cell proliferation assay

In total, 3000 MEFs were seeded in each well in 96-well plates and transduced with 4F virus and shRNA lentivirus (or transfected with miRNA inhibitors). Starting from day 1 post-transduction/transfection, every 2 days, cells were incubated with mES medium containing Celltiter 96 Aqueous one solution (Promega, G3580) for 1 h in tissue culture incubator. Absorbance at 490 nm was then measured for each well using plate reader and collected data were used to generate relative proliferation curve using signal from day 1 post-transduction/transfection as the reference.

Supplementary data

Supplementary data are available at *The EMBO Journal* Online (http://www.embojournal.org).

Acknowledgements

We thank Mark Mercola, Evan Snyder and Rana laboratory members for helpful discussions and support. We are grateful for the following shared resource facilities at the Sanford-Burnham Institute: genomics and informatics and data management core for miRNA and mRNA array experiments and data analysis; the animal facility for the generation of teratomas and chimeric mice; and the histology and molecular pathology core for characterization of various tissues.

Conflict of interest

The authors declare that they have no conflict of interest.

References

Abbas T, Dutta A (2009) p21 in cancer: intricate networks and multiple activities. *Nat Rev Cancer* **9:** 400–414

Ambros V (2004) The functions of animal microRNAs. *Nature* **431:** 350–355

Aoi T, Yae K, Nakagawa M, Ichisaka T, Okita K, Takahashi K, Chiba T, Yamanaka S (2008) Generation of pluripotent stem cells from adult mouse liver and stomach cells. *Science* **321:** 699–702

Banito A, Rashid ST, Acosta JC, Li S, Pereira CF, Geti I, Pinho S, Silva JC, Azuara V, Walsh M, Vallier L, Gil J (2009) Senescence impairs successful reprogramming to pluripotent stem cells. *Genes Dev* **23:** 2134–2139

Bartel DP (2004) MicroRNAs: genomics, biogenesis, mechanism, and function. *Cell* **116:** 281–297

Blelloch R, Wang Z, Meissner A, Pollard S, Smith A, Jaenisch R (2006) Reprogramming efficiency following somatic cell nuclear

transfer is influenced by the differentiation and methylation state of the donor nucleus. *Stem Cells* **24:** 2007–2013

Eminli S, Utikal J, Arnold K, Jaenisch R, Hochedlinger K (2008) Reprogramming of neural progenitor cells into induced pluripotent stem cells in the absence of exogenous Sox2 expression. *Stem Cells* **26:** 2467–2474

Gartel AL, Ye X, Goufman E, Shianov P, Hay N, Najmabadi F, Tyner AL (2001) Myc represses the p21(WAF1/CIP1) promoter and interacts with Sp1/Sp3. *Proc Natl Acad Sci USA* **98:** 4510–4515

Giorgetti A, Montserrat N, Aasen T, Gonzalez F, Rodriguez-Piza I, Vassena R, Raya A, Boue S, Barrero MJ, Corbella BA, Torrabadella M, Veiga A, Izpisua Belmonte JC (2009) Generation of induced pluripotent stem cells from human cord blood using OCT4 and SOX2. *Cell Stem Cell* **5:** 353–357

Greber B, Lehrach H, Adjaye J (2007) Fibroblast growth factor 2 modulates transforming growth factor beta signaling in mouse embryonic fibroblasts and human ESCs (hESCs) to support hESC self-renewal. *Stem Cells* **25:** 455–464

Hanna J, Markoulaki S, Schorderet P, Carey BW, Beard C, Wernig M, Creyghton MP, Steine EJ, Cassady JP, Foreman R, Lengner CJ, Dausman JA, Jaenisch R (2008) Direct reprogramming of terminally differentiated mature B lymphocytes to pluripotency. *Cell* **133:** 250–264

Hong H, Takahashi K, Ichisaka T, Aoi T, Kanagawa O, Nakagawa M, Okita K, Yamanaka S (2009) Suppression of induced pluripotent stem cell generation by the p53-p21 pathway. *Nature* **460:** 1132–1135

Houbaviy HB, Murray MF, Sharp PA (2003) Embryonic stem cell-specific microRNAs. *Dev Cell* **5:** 351–358

Hutvagner G, Simard MJ, Mello CC, Zamore PD (2004) Sequence-specific inhibition of small RNA function. *PLoS Biol* **2:** E98

Ichida JK, Blanchard J, Lam K, Son EY, Chung JE, Egli D, Loh KM, Carter AC, Di Giorgio FP, Koszka K, Huangfu D, Akutsu H, Liu DR, Rubin LL, Eggan K (2009) A small-molecule inhibitor of Tgf-beta signaling replaces Sox2 in reprogramming by inducing nanog. *Cell Stem Cell* **5:** 491–503

Ivanovska I, Ball AS, Diaz RL, Magnus JF, Kibukawa M, Schelter JM, Kobayashi SV, Lim L, Burchard J, Jackson AL, Linsley PS, Cleary MA (2008) MicroRNAs in the miR-106b family regulate p21/CDKN1A and promote cell cycle progression. *Mol Cell Biol* **28:** 2167–2174

Judson RL, Babiarz JE, Venere M, Blelloch R (2009) Embryonic stem cell-specific microRNAs promote induced pluripotency. *Nat Biotechnol* **27:** 459–461

Kahlem P, Newfeld SJ (2009) Informatics approaches to understanding TGFbeta pathway regulation. *Development* **136:** 3729–3740

Kawamura T, Suzuki J, Wang YV, Menendez S, Morera LB, Raya A, Wahl GM, Belmonte JC (2009) Linking the p53 tumour suppressor pathway to somatic cell reprogramming. *Nature* **460:** 1140–1144

Kim VN, Han J, Siomi MC (2009a) Biogenesis of small RNAs in animals. *Nat Rev Mol Cell Biol* **10:** 126–139

Kim YK, Yu J, Han TS, Park SY, Namkoong B, Kim DH, Hur K, Yoo MW, Lee HJ, Yang HK, Kim VN (2009b) Functional links between clustered microRNAs: suppression of cell-cycle inhibitors by microRNA clusters in gastric cancer. *Nucleic Acids Res* **37:** 1672–1681

Lal A, Navarro F, Maher CA, Maliszewski LE, Yan N, O'Day E, Chowdhury D, Dykxhoorn DM, Tsai P, Hofmann O, Becker KG, Gorospe M, Hide W, Lieberman J (2009) miR-24 inhibits cell proliferation by targeting E2F2, MYC, and other cell-cycle genes via binding to 'seedless' 3′UTR microRNA recognition elements. *Mol Cell* **35:** 610–625

Landgraf P, Rusu M, Sheridan R, Sewer A, Iovino N, Aravin A, Pfeffer S, Rice A, Kamphorst AO, Landthaler M, Lin C, Socci ND, Hermida L, Fulci V, Chiaretti S, Foa R, Schliwka J, Fuchs U, Novosel A, Muller RU *et al* (2007) A mammalian microRNA expression atlas based on small RNA library sequencing. *Cell* **129:** 1401–1414

Latronico MV, Condorelli G (2009) MicroRNAs and cardiac pathology. *Nat Rev Cardiol* **6:** 419–429

Li H, Collado M, Villasante A, Strati K, Ortega S, Canamero M, Blasco MA, Serrano M (2009a) The Ink4/Arf locus is a barrier for iPS cell reprogramming. *Nature* **460:** 1136–1139

Li R, Liang J, Ni S, Zhou T, Qing X, Li H, He W, Chen J, Li F, Zhuang Q, Qin B, Xu J, Li W, Yang J, Gan Y, Qin D, Feng S, Song H, Yang D, Zhang B *et al* (2010) A mesenchymal-to-epithelial transition initiates and is required for the nuclear reprogramming of mouse fibroblasts. *Cell Stem Cell* **7:** 51–63

Li W, Wei W, Zhu S, Zhu J, Shi Y, Lin T, Hao E, Hayek A, Deng H, Ding S (2009b) Generation of rat and human induced pluripotent stem cells by combining genetic reprogramming and chemical inhibitors. *Cell Stem Cell* **4:** 16–19

Lowry WE, Richter L, Yachechko R, Pyle AD, Tchieu J, Sridharan R, Clark AT, Plath K (2008) Generation of human induced pluripotent stem cells from dermal fibroblasts. *Proc Natl Acad Sci USA* **105:** 2883–2888

Lyssiotis CA, Foreman RK, Staerk J, Garcia M, Mathur D, Markoulaki S, Hanna J, Lairson LL, Charette BD, Bouchez LC, Bollong M, Kunick C, Brinker A, Cho CY, Schultz PG, Jaenisch R (2009) Reprogramming of murine fibroblasts to induced pluripotent stem cells with chemical complementation of Klf4. *Proc Natl Acad Sci USA* **106:** 8912–8917

Maherali N, Hochedlinger K (2009) Tgfbeta signal inhibition cooperates in the induction of iPSCs and replaces Sox2 and cMyc. *Curr Biol* **19:** 1718–1723

Makeyev EV, Zhang J, Carrasco MA, Maniatis T (2007) The MicroRNA miR-124 promotes neuronal differentiation by triggering brain-specific alternative pre-mRNA splicing. *Mol Cell* **27:** 435–448

Meissner A, Wernig M, Jaenisch R (2007) Direct reprogramming of genetically unmodified fibroblasts into pluripotent stem cells. *Nat Biotechnol* **25:** 1177–1181

Meister G, Landthaler M, Dorsett Y, Tuschl T (2004) Sequence-specific inhibition of microRNA- and siRNA-induced RNA silencing. *RNA* **10:** 544–550

Mendell JT (2008) miRiad roles for the miR-17-92 cluster in development and disease. *Cell* **133:** 217–222

Mikkelsen TS, Hanna J, Zhang X, Ku M, Wernig M, Schorderet P, Bernstein BE, Jaenisch R, Lander ES, Meissner A (2008) Dissecting direct reprogramming through integrative genomic analysis. *Nature* **454:** 49–55

Moustakas A, Heldin CH (2009) The regulation of TGFbeta signal transduction. *Development* **136:** 3699–3714

Nakagawa M, Koyanagi M, Tanabe K, Takahashi K, Ichisaka T, Aoi T, Okita K, Mochiduki Y, Takizawa N, Yamanaka S (2008) Generation of induced pluripotent stem cells without Myc from mouse and human fibroblasts. *Nat Biotechnol* **26:** 101–106

Ogawa K, Saito A, Matsui H, Suzuki H, Ohtsuka S, Shimosato D, Morishita Y, Watabe T, Niwa H, Miyazono K (2007) Activin-Nodal signaling is involved in propagation of mouse embryonic stem cells. *J Cell Sci* **120:** 55–65

Park IH, Zhao R, West JA, Yabuuchi A, Huo H, Ince TA, Lerou PH, Lensch MW, Daley GQ (2008) Reprogramming of human somatic cells to pluripotency with defined factors. *Nature* **451:** 141–146

Rana TM (2007) Illuminating the silence: understanding the structure and function of small RNAs. *Nat Rev Mol Cell Biol* **8:** 23–36

Samavarchi-Tehrani P, Golipour A, David L, Sung HK, Beyer TA, Datti A, Woltjen K, Nagy A, Wrana JL (2010) Functional genomics reveals a BMP-driven mesenchymal-to-epithelial transition in the initiation of somatic cell reprogramming. *Cell Stem Cell* **7:** 64–77

Seoane J, Le HV, Massague J (2002) Myc suppression of the p21(Cip1) Cdk inhibitor influences the outcome of the p53 response to DNA damage. *Nature* **419:** 729–734

Shi Y, Desponts C, Do JT, Hahm HS, Scholer HR, Ding S (2008a) Induction of pluripotent stem cells from mouse embryonic fibroblasts by Oct4 and Klf4 with small-molecule compounds. *Cell Stem Cell* **3:** 568–574

Shi Y, Do JT, Desponts C, Hahm HS, Scholer HR, Ding S (2008b) A combined chemical and genetic approach for the generation of induced pluripotent stem cells. *Cell Stem Cell* **2:** 525–528

Sridharan R, Tchieu J, Mason MJ, Yachechko R, Kuoy E, Horvath S, Zhou Q, Plath K (2009) Role of the murine reprogramming factors in the induction of pluripotency. *Cell* **136:** 364–377

Takahashi K, Tanabe K, Ohnuki M, Narita M, Ichisaka T, Tomoda K, Yamanaka S (2007) Induction of pluripotent stem cells from adult human fibroblasts by defined factors. *Cell* **131:** 861–872

Takahashi K, Yamanaka S (2006) Induction of pluripotent stem cells from mouse embryonic and adult fibroblast cultures by defined factors. *Cell* **126:** 663–676

Tay Y, Zhang J, Thomson AM, Lim B, Rigoutsos I (2008) MicroRNAs to Nanog, Oct4 and Sox2 coding regions modulate embryonic stem cell differentiation. *Nature* **455:** 1124–1128

Utikal J, Polo JM, Stadtfeld M, Maherali N, Kulalert W, Walsh RM, Khalil A, Rheinwald JG, Hochedlinger K (2009) Immortalization eliminates a roadblock during cellular reprogramming into iPS cells. *Nature* **460:** 1145–1148

Vermeulen A, Robertson B, Dalby AB, Marshall WS, Karpilow J, Leake D, Khvorova A, Baskerville S (2007) Double-stranded regions are essential design components of potent inhibitors of RISC function. *RNA* **13:** 723–730

Wang WX, Wilfred BR, Xie K, Jennings MH, Hu YH, Stromberg AJ, Nelson PT (2010) Individual microRNAs (miRNAs) display distinct mRNA targeting 'rules'. *RNA Biol* **7:** 373–380

Wang Y, Baskerville S, Shenoy A, Babiarz JE, Baehner L, Blelloch R (2008) Embryonic stem cell-specific microRNAs regulate the G1-S transition and promote rapid proliferation. *Nat Genet* **40:** 1478–1483

Xu N, Papagiannakopoulos T, Pan G, Thomson JA, Kosik KS (2009) MicroRNA-145 regulates OCT4, SOX2, and KLF4 and represses pluripotency in human embryonic stem cells. *Cell* **137:** 647–658

Yu J, Vodyanik MA, Smuga-Otto K, Antosiewicz-Bourget J, Frane JL, Tian S, Nie J, Jonsdottir GA, Ruotti V, Stewart R, Slukvin II, Thomson JA (2007) Induced pluripotent stem cell lines derived from human somatic cells. *Science* **318:** 1917–1920

